Role of retained austenite in low alloy steel at low temperature monitored by neutron diffraction

Takayuki Yamashita[1,*], Satoshi Morooka[1], Stefanus Harjo[1], Takuro Kawasaki[1], Norimitsu Koga[2], Osamu Umezawa[3]

[1] *J-PARC center, Japan Atomic Energy Agency, 2-4 Shirakata, Tokai, Naka, Ibaraki, 319-1195, Japan*

[2] *Faculty of Mechanical Engineering, Kanazawa University, Kakumamachi, Kanazawa, Ishikawa, 920-1192, Japan*

[3] *Faculty of Engineering, Yokohama National University, 79-5 Tokiwadai, Hodogaya, Yokohama, 240-8501, Japan*

ABSTRACT

In-situ neutron diffraction measurements during tensile tests at low temperatures of a low alloy steel containing retained austenite (γ) have been performed. Evolutions of phase fractions and phase stresses were analyzed and discussed with the progress of deformation. The role of γ in the steel during deformation at low temperatures was observed not to directly in the contribution to the strengths but in the improvement of the elongation by transformation of γ to martensite -and in the increasing of the work-hardening rate by an increase in the phase fraction of martensite and the work hardening of martensite.

Keywords: Martensitic transformation, low alloy steel, neutron diffraction, phase stress, phase fraction

*Corresponding author, E-mail: yamashi@post.j-parc.jp

Transformation-induced plasticity (TRIP) is one of important effects to enhance strength and ductility in low alloy steel, as results of the transformation from metastable retained austenite (γ) to martensite (α') (martensitic transformation) induced by deformation [1-4]. The mechanical stability of γ closely affects the behavior of TRIP. Sugimoto et. al. [5] reported that a low alloy steel containing metastable γ showed excellent total elongation above 50 % strain at 423 K, where austenite was in a stable condition. Not only test temperature [5,6], but also carbon concentration [7], morphology [8-10] and precipitation cite [10,11] of γ are significant factors for the stability. On the other hand, there are few reports on the stability of γ and deformation induced martensitic transformation at low temperatures. In our previous study [12], we investigated tensile properties and changes of phase fraction of γ in a low alloy TRIP steel deformed at low temperatures using electron back scattered diffraction (EBSD) method, and discussed the mechanical properties and martensitic transformation behavior under low temperature. A good balance of strength and ductility appeared in a temperature range from 193 K to 293 K due to a high work-hardening rate in the initial stage of deformation and the strengthening of bainitic ferrite matrix by lowering temperature. We suggested that γ contributed to the high work-hardening rate by deformation induced martensitic transformation, but there was no a direct proof showing evolutions of stresses of γ and α' during deformation. A reason why the steel showed the excellent elongation at low temperature deformation was also not clear yet because the counting loss of γ with small grain size (~ 1 μm) might occur in EBSD measurement. Thus, it's desirable to observe accurately the transformation behavior of γ at low temperatures.

In-situ neutron diffraction during tensile deformation has been proved to be one of appropriate methods for simultaneous evaluations of phase stresses and phase fractions of constituent phases in TRIP steels [13-16]. Not only the phase stresses of ferrite matrix and γ, but also the α' phase stress has been estimated [15,16]. Blonde et. al. investigated the temperature dependent mechanical stability of austenite in a low alloy steel using high energy X-ray diffraction [17]. They revealed that the transformation amount of austenite was about 50 % at low temperatures, and the transformation progressed gradually during deformation. However, the strengthening of bainitic ferrite matrix and stress partitioning behavior among the constituent phases were not evaluated yet.

In the present study, the changes of phase fractions and phase stresses of constituent phases (ferrite and bainite matrix, γ and α') in a low alloy steel during tensile loading at low temperatures were evaluated using *in-situ* neutron diffraction, and the stability of γ, deformation induced martensitic transformation behavior (or TRIP effect) and the contribution to the strength are discussed.

A steel plate of 0.31C-1.74Si-1.49Mn (in mass%) was cold-rolled and annealed at 1063 K (region of two phases of ferrite and austenite) for 400 s, and then austempered at 673 K for 600 s. A typical SEM micrograph of the steel before deformation is shown in Fig.1(a). The steel consists of ferrite, bainite and γ. The shape of tensile test specimen is shown in Fig. 1(b). Plate type specimens with a

thickness of 2.5 mm were prepared using an electric discharged cutting method, in which the longitudinal direction (loading axial direction) to be parallel to the rolling direction. The specimens' surface was ground using SiC emery papers up to 1200 grid, and then electropolished in a stirred solution of perchloric acid and ethanol at 253 K and 31 V for 60 s.

In-situ neutron diffraction measurement during tensile test at low temperature was carried out using "TAKUMI [18]" a time-of-flight engineering materials diffractometer at MLF of J-PARC. The test temperatures were 293 K, 233 K, 193 K and 134 K, which were controlled by a liquid nitrogen cooling system equipment [19]. The temperature was monitored using thermocouple attached on the specimen at the grip parts. The schematic experimental setup is shown in Fig. 1(c), where the tensile loading machine was aligned in such a way that the loading axis to be horizontally 45 degree with respect to the incident neutron beam. Macroscopic strains were measured by an extensometer at 293 K and a strain gage at low temperature. The neutron diffraction data for the scattering vector parallel to the axial direction was collected at the axial detector, while the data for the scattering vector perpendicular to the loading axis (transverse direction) at the transverse detector. The size of incident beam slit was 5 mm × 5mm, and a pair of radial collimators viewing 5 mm width was adopted. The proton beam power for the neutron diffraction measurement was 300 kW. The tensile test was done by a step-increasing load control with 300 s holding time in the elastic region and by a continues crosshead speed control (with the initial strain rate of 1.3×10^{-5} s^{-1}) in the plastic region. The data for the plastic region was then sliced per 300 s or 600 s. The measurements were performed up to the ultimate tensile strengths (UTS). In this paper, ferrite and bainite was assumed to be the same phase of a bainitic ferrite (α) because the peak separation between ferrite and bainite was difficult. Peak separation between α and α' was conducted by assuming that the c/a ratio of α' was constant during whole deformation and could be simplified by a single-broad BCC peak.

The nominal stress-nominal strain curves and the work-hardening rate with respect to the true strain obtained at different test temperatures are presented in Fig. 2(a) and (b), respectively. The steel exhibited good balances of tensile strength and homogeneous elongation at 193 K, 233 K and 293 K, which are in good agreement with our previous study [12]. However, the specimen fractured at a relatively lower applied true strain during tensile test at 134 K. Stress fluctuations appeared in the nominal stress-nominal strain curve for tensile test at 293 K indicated by arrows in Fig. 2(a). These fluctuations might be related to a dynamic strain aging [20,21], which are not observed at low temperature tests in the present study or a tensile test at room temperature with a higher strain rate of 2.8×10^{-4} s^{-1} in our previous study [12].

The lattice constants were obtained by Pawley refinement using a software called "Z-Rietveld" [22]. The phase fractions of γ were obtained by Rietveld refinement using the same software and the values determined from the diffraction pattern in the axial direction and that in the transverse direction were then averaged to minimize the influence of texture. The carbon concentration in γ

(X_C^γ) was estimated from the lattice constants of γ ($a_{\gamma,0}$) and α ($a_{\alpha,0}$) averaged respectively for the axial and the transverse directions before deformation according to the empirical equation (1) [23].

$$X_C^\gamma = \left(a_{\gamma,0} - 3.572/2.8664 \cdot a_{\alpha,0}\right)/0.033 \qquad (1)$$

The estimated X_C^γ was 1.34 mass%.

The changes of phase fraction of γ (f_γ) during tensile deformation at various test temperatures are shown in Fig. 2(c). The f_γ values before deformation were 20.2% at 293 K, 19.6% at 233 K, 19.8% at 193 K and 19.0% at 134 K, respectively. Though a small amount of γ grains might transform to α'. γ was quite stable during cooling to 134 K. The martensitic transformation mostly occurred after macroscopic yielding at each test temperature. At 293 K, the f_γ value decreased almost lineally with increasing the applied true strain. The f_γ value remained when the deformation at 293 K reached the UTS was approximately 7.2 vol%. The f_γ value decreased with a higher rate and remained with a lower value by lowering tensile test temperature. The f_γ values remained at the end of deformation were 3.8% at 233 K, 2.8% at 193 K and 2.2% at 134 K, respectively. In our previous study [12], from EBSD method almost all γ transformed to α' in tensile test at low temperatures when the applied strain reached about 10%. These differences might be due to the conditions that EBSD method has a low accuracy for counting small grains. It can be suggested that the fine γ grains remained at the end of deformation at low temperatures and the martensitic transformation occurred continuously until the specimen fractured. The TRIP effect therefore is confirmed to contribute to the good balance of strength and ductility at 134 K, 193 K and 233 K.

Phase average lattice strains ($\varepsilon_i^{ave}, i = \alpha, \gamma$ and α') were estimated according to Eq. (2).

$$\varepsilon_i^{ave} = (a_i - a_{i,0})/a_{i,0} \qquad (2)$$

where a_i is the lattice constant obtained during deformation and $a_{i,0}$ is the reference lattice constant or that before deformation in this case. At low temperatures, the $a_{i,0}$ values were the lattice constant measured at the same temperatures before deformation. Phase stresses were then evaluated from the ε_i^{ave} values according to Eq. (3) [15].

$$\sigma_i = E_i\, \varepsilon_i^{ave} \qquad (3)$$

Here E_i ($i = \alpha, \gamma$ and α') is Young's moduli for α matrix, γ and α', respectively. The values of E_γ= 200 GPa and $E_\alpha = E_{\alpha'}$ = 210 GPa were used in these calculations.

The lattice constant of α' before loading, *i.e.* $a_{\alpha' 0}$ is needed to calculate the values of $\varepsilon_{\alpha'}^{ave}$ and $\sigma_{\alpha'}$. Here, we tried to use a stress equilibrium approach to determine the $a_{\alpha' 0}$. That is, the sum of phase stresses -weighted by their phase fractions must be equal to the applied true stress (σ_{app}) in a loaded state, according to Eq. (4):

$$f_\alpha \sigma_\alpha + f_\gamma \sigma_\gamma + f_{\alpha'} \sigma_{\alpha'} = \sigma_{app} \qquad (4)$$

Here f_i (i is α, γ and α') is phase fraction. The $\sigma_{\alpha'}$ value in a loaded state could be evaluated because the values of f_α, f_γ, $f_{\alpha'}$, σ_α, σ_γ and σ_{app} were known. The values of $\varepsilon_{\alpha'}^{ave}$ were then calculated according Eq. (3), and $a_{\alpha',0}$ could be evaluated. All conditions since the f_γ values

decreased by deformation were used in these calculations, and the averaged $a_{\alpha'0}$ value was determined. The $a_{\alpha'0}$ value for each test temperature was determined independently.

Figure 3 shows the values of σ_α, σ_γ and $\sigma_{\alpha'}$ as a function of applied true stress at four test temperature. It is noticed that α' bears the highest phase stresses among the constituent phases during deformation at four test temperatures. The $\sigma_{\alpha'}$ values are larger than 2 GPa which are in good agreement with previous studies using low alloy steels with the TRIP effects [15,16]. The $\sigma_{\alpha'}$ values increased with increasing the applied true stresses. The σ_γ values, at the beginning of plastic deformation (in the elasto-plastic region and before α' appears), are larger than the σ_α values showing that γ shed larger stresses than α matrix, i.e. α matrix starts plastic deformation preferentially. This situation is clearly observed at 293 K. When γ yielded the martensitic transformation seemed to start in the same time. The partitioning at the beginning of plastic deformation between σ_α and σ_γ becomes smaller with decreasing the test temperature, that may be due to a decrease in the threshold of σ_γ for the martensitic transformation by decreasing temperature. In addition, the austenite phase stress was almost constant for applied true stress after start to plastic deformation of austenite. It suggested that the martensitic transformation of austenite under low temperatures prior to plastic deformation of austenite when phase stress of austenite reach threshold stress level.

By weighting the σ_i with the f_i of each phase, a contributed stress to the strength (contributed stress) of each phase can be evaluated. The contributed stresses of α matrix, γ and α' as a function of applied true strain during tensile tests at various test temperatures are shown in Fig. 4. The contributed stress of α matrix is higher than the other phases at early stage of deformation due to its large phase fraction. It increases with deformation due to its work hardening that can be understood from the increase in the $\sigma_{\alpha'}$. The contributed stress of α' is very low at early stage of deformation though the $\sigma_{\alpha'}$ value is very high from the state where α' is formed, as shown in Fig. 3. The main reason is because the amount of α' at early stage of deformation is small. The contributed stress of α' is enhanced by the progressing of deformation due to the increase in the $f_{\alpha'}$ and the work hardening of α' which can be understood by the increase in the $\sigma_{\alpha'}$ (see Fig. 3). The contributed stress of α' is enhanced also by decreasing temperature. At each test temperature, the portions of contributed stresses of α matrix and α' are almost similar at the end of deformation. The contributed stresses of γ decrease by the progressing of deformation due to decreases in the f_γ as results of continuous martensitic transformation with the deformation. The difference in the portion of contributed stress of γ at the end of deformation is mainly reflected by the difference in the f_γ remained. It is noticed also that the σ_γ values are almost constant in the plastic region (after γ start the martensitic transformation) during deformation at low temperatures (see Fig. 3). Especially, during deformation at 193 K and 134 K, the small values of f_γ and the unchanged σ_γ values in the plastic region result in very low contributed stresses of γ at later stage of deformation (above 15% applied true strain).

The γ has almost no contribution to the strength at later stage of deformation (above 15% applied true strain) at 193 K and 134 K.

In summary, the martensitic transformation occurred gradually with deformation. The stress contributions to the strength of α matrix and α' become large at later stage of deformation, while, that of γ decreases. During deformation at low temperatures, γ has almost no contribution to the strength due to the decrease in the phase fraction and the unchanged σ_γ values in the plastic region. The role of γ in the steel used in this study at low temperature deformation can be understood not to directly in the contribution to the stress but in the improvement of the elongation by TRIP effect and in the increasing of the work-hardening rate by promoting the martensitic transformation.

Acknowledgement

The neutron diffraction experiments were performed at BL19 in Materials and Life Science Experimental Facility of J-PARC with the proposals of 2016P0200, and got partly financial supports from the Japan Society for the Promotion of Science No. 15H05767 and No. 19K15279.

References

[1] Tamura, Metal Sci. 16 (1982) 245-253.

[2] H. K. D. H. Bhadeshia, ISIJ Int. 42 (2002) 1059-1060.

[3] P. J. Jacques, Curr. Opin. Solid State Mater. Sci. 8 (2004) 259-265.

[4] B. C. De Cooman, Curr. Opin. Solid State Mater. Sci. 8(2004) 285-303.

[5] K. Sugimoto, M. Kobayashi, S. Hashimoto, Metall. Mater. Trans. A, 23A (1992) 3085-3091.

[6] O. Muránsky, P. Šittner, J. Zrník, E. C. Oliver, Acta Mater. 56 (2008) 3367-3379.

[7] A. Itami, M. Takahashi, K. Ushioda, ISIJ Int. 35 (1995) 1121-1127.

[8] K. Sugimoto, M. Misu, M. Kobayashi, H. Shirasawa, ISIJ Int. 33 (1993) 775-782.

[9] M. Mukherjee, O. N. Mohanty, S. Hashimoto, T. Hojo, K. Sugimoto, ISIJ Int. 46 (2006) 316-324.

[10] G.K. Tirumalasetty, M.A. van Huis, C. Kwakernaak, J. Sietsma, W.G. Sloof, H.W. Zandbergen, Acta Mater. 60 (2012) 1311-1321.

[11] H. Matsuda, H. Noro, Y. Nagataki, Hosoya, Mater. Sci. Forum 638-642 (2010) 3374-3379.

[12] T. Yamashita, N. Koga, O. Umezawa, ISIJ Int. 58 (2018) 1155-1161.

[13] K. Asoo, Y. Tomota, S. Harjo, Y. Okitsu, ISIJ Int. 51 (2011) 145-150.

[14] O. Muránsky, P. Horňak, P. Lukáš, J. Zrník, P. Šittner, J. Achiev. Mater. Manuf. Eng. 14 (2006) 26-30.

[15] S. Harjo, N. Tsuchida, J. Abe, W. Gong, Sci. rep. 7 (2017) 15149.

[16] P. J. Jacques, Q. Furnemont, S. Godet, T. Pardoen, K. T. Conlon, F. Delannay, Philos. Mag. 86 (2006) 2371-2392.

[17] R. Blondé, E. Jimenez-Melero, L. Zhao, J.P. Wright, E. Brück, S. van der Zwaag, N.H. van Dijk, Acta Mater. 60 (2012) 565-577.

[18] S. Harjo, T. Ito, K. Aizawa, H. Arima, J. Abe, A. Moriai, T. Iwahashi, T. Kamiyama, Mater. Sci. Forum, 681 (2011), 443-448.

[19] S. Harjo, K. Aizawa, T. Kawasaki, T. Iwahashi, T. Nakamoto, T. Henmi, Proceedings of the 21st Meeting of the International Collaboration on Advanced Neutron Sources, ed. by T. Oku, M. Nakamura, K. Sakai, M. Teshigawara, H. Hatsumoto, M. Yonemura, J. Suzuki, M. Arai, Ibaraki, Japan, 2016, 441-447.

[20] Y. Nakada, A. S. Keh, Acta Metall. 18 (1970), 437-443.

[21] M. Koyama, T. Sawaguchi, K. Tsuzaki, ISIJ Int. 58 (2018), 1383-1395.

[22] R. Oishi, M. Yonemura, Y. Nishimaki, S. Torii, A. Hoshikawa, T. Ishigaki, T. Morishima, K. Mori, T. Kamiyama, Nucl. Instr. Methods Phys. Res. A 600 (2009), 94-96.

[23] L. Cheng, A. Bottger, Th.H. de Keijse, E.J. Mittemeijer, Scr. Metall. Mater. 24 (1990) 509-514.

Caption list

Figure 1 (a) initial microstructure of the test steel before deformation, (b) shape of the tensile test specimen in this study and (c) schematic experimental setup of TAKUMI instrument. The white arrows in (a) indicate retained austenite as an example.

Figure 2 (a) Nominal stress – nominal strain curves, (b) true stress and work-hardening rate vs. true strain and (c) phase fraction of retained austenite as a function of true strain at various test temperatures. The black arrows in (a) indicate stress fluctuations.

Figure 3 Phase stresses of bainitic ferrite, austenite and martensite at (a) 293 K, (b) 233 K, (c) 193 K and (d) 134 K with respect to applied true stress. The phase stresses of ferrite + bainite (α matrix), austenite and martensite are colored with red, green and blue, respectively. The solid black line in figures indicates applied true stress at various test temperatures.

Figure 4 The changes of fraction weighted phase stresses of each consisting phases during tensile at (a) 293 K, (b) 233 K, (c) 193 K and (d) 134 K. The applied true stress-strain curves are superimposed. Those for bainitic ferrite (α matrix), austenite and martensite are colored with red, green and blue, respectively.

Figure(s)

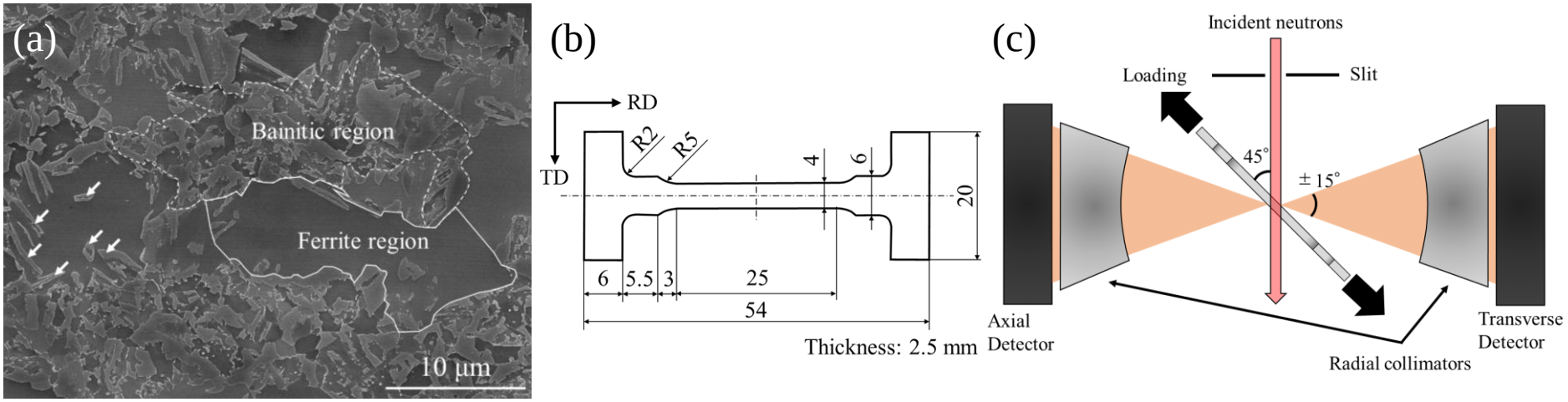

Figure 1 (a) initial microstructure of the test steel before deformation, (b) shape of the tensile test specimen in this study and (c) schematic experimental setup of TAKUMI instrument. The white arrows in (a) indicate retained austenite as an example.

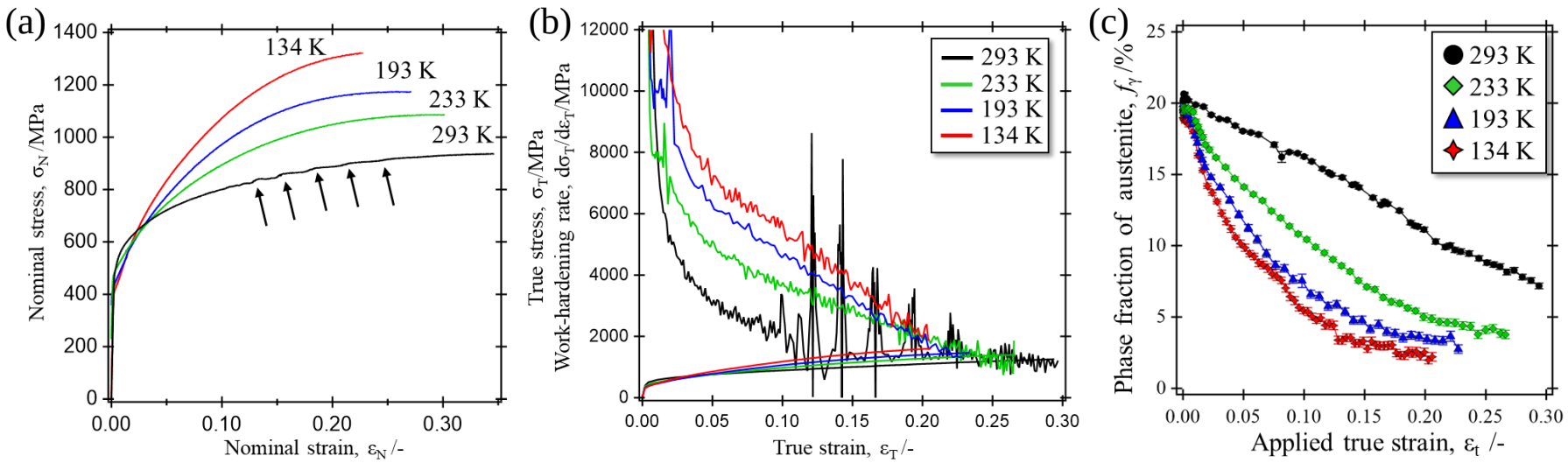

Figure 2 (a) Nominal stress – nominal strain curves, (b) true stress and work-hardening rate vs. true strain and (c) phase fraction of retained austenite as a function of true strain at various test temperatures. The black arrows in (a) indicate stress fluctuations.

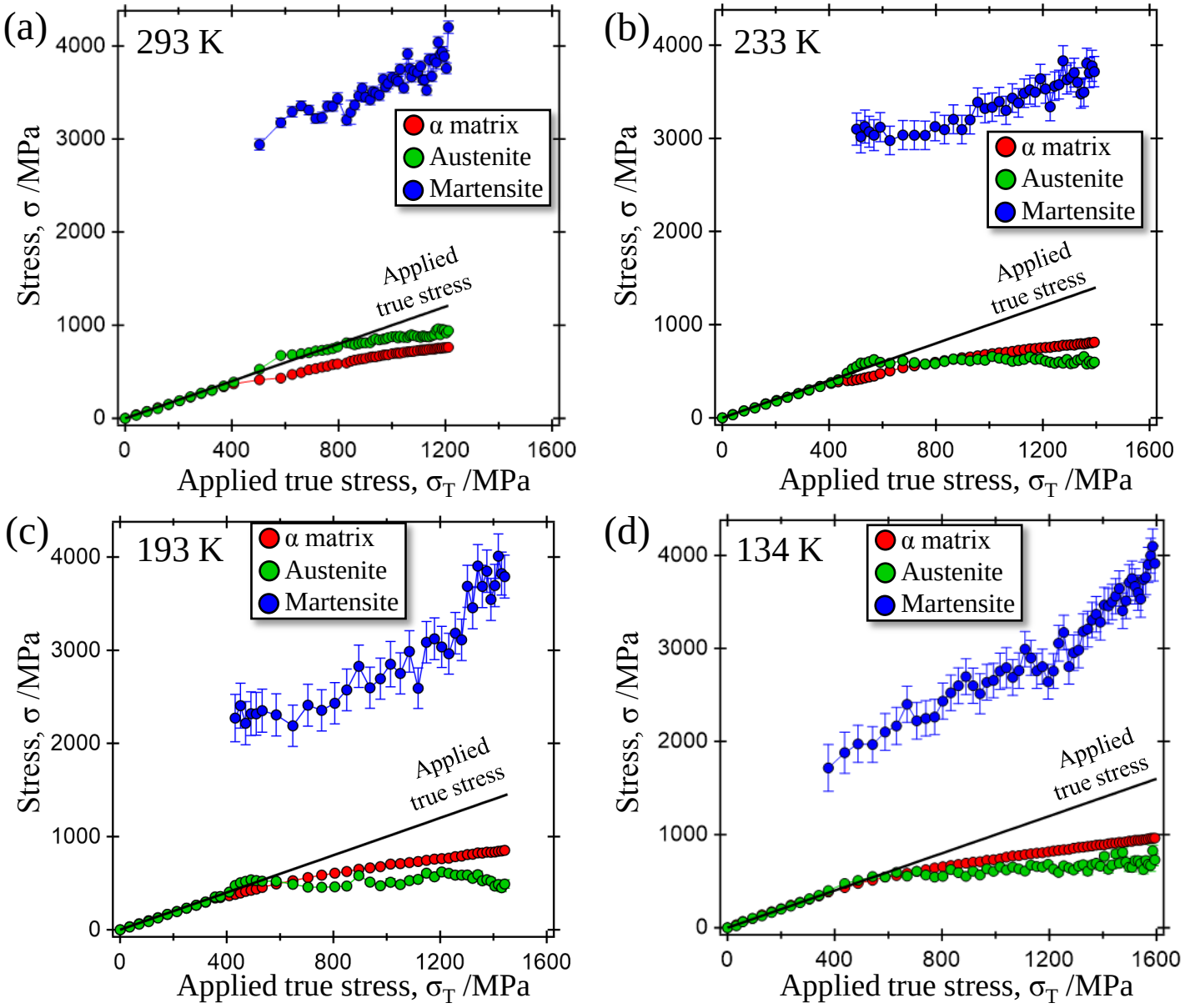

Figure 3 Phase stresses of bainitic ferrite, austenite and martensite at (a) 293 K, (b) 233 K, (c) 193 K and (d) 134 K with respect to applied true stress. The phase stresses of ferrite + bainite (α matrix), austenite and martensite are colored with red, green and blue, respectively. The solid black line in figures indicates applied true stress at various test temperatures.

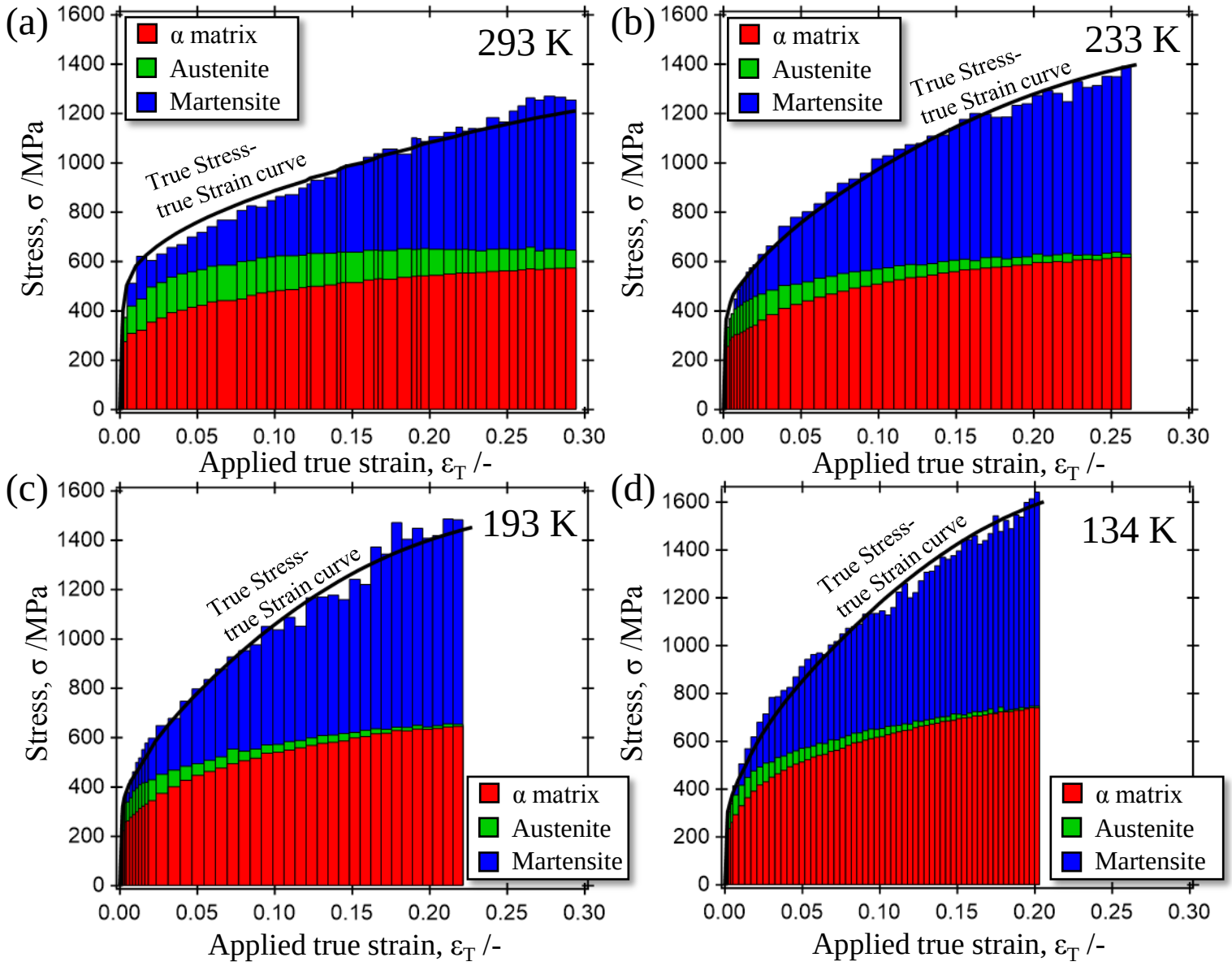

Figure 4 The changes of fraction weighted phase stresses of each consisting phases during tensile at (a) 293 K, (b) 233 K, (c) 193 K and (d) 134 K. The applied true stress-strain curves are superimposed. Those for bainitic ferrite (α matrix), austenite and martensite are colored with red, green and blue, respectively.

Graphical Abstract